FZJ SC CAVITY COUPLED ANALYSIS

E. Zaplatin, FZJ, Juelich, Germany

Abstract

A sequential coupled field analysis Thermal/Structural/RF is used to predict the frequency drift of three types of superconducting cavities (500 MHz, β = 0.75 – elliptic cavity, 160 MHz, β = 0.11 – half-wave resonator, 760 MHz, β = 0.2 – triple-spoke cavity), which are under investigations at Forschungszentrum Juelich. The resonant cavity frequency is affected by the deformations of its shape due to the atmospheric pressure, cavity cool-down, Lorenz forces and tuning force. The factors that define the accuracy of these analyses are discussed. The results of simulations are compared with experimental data.

Contribution to the SRF'05, Ithaca, New York, USA

Work supported by the European Community-Research Infrastructure Activity under the FP6 "Structuring the European Research Area" programme (CARE, contract number RII3-CT-2003-506395).

FZJ SC CAVITY COUPLED ANALYSIS

E. Zaplatin, FZJ, Juelich, Germany

Abstract

A sequential coupled field analysis Thermal/Structural/RF is used to predict the frequency drift of three types of superconducting cavities (500 MHz, $\beta = 0.75$ – elliptic cavity, 160 MHz, $\beta = 0.11$ – half-wave resonator, 760 MHz, $\beta = 0.2$ – triple-spoke cavity), which are under investigations at Forschungszentrum Juelich. The resonant cavity frequency is affected by the deformations of its shape due to the atmospheric pressure, cavity cool-down, Lorenz forces and tuning force.

The factors that define the accuracy of these analyses are discussed. The results of simulations are compared with experimental data.

1 ELLIPTICAL CAVITY

Some additional features of the specialized RF codes like MAFIA, MWS, HFSS [1-2] (for instance a number of specific macros), favour to use these programs for cavity RF parameter optimizations. On the other hand, the existence of the RF code in ANSYS [3] together with ability to use the same meshed model and exchange the results between different types of simulations promises the better final results. It means the main task of electrodynamics' simulation in ANSYS is to receive the results as close as possible to the specialized RF codes. Since the further simulations of the structure will be related and normalized on the peak fields found, the solution of the proper field distribution on the surface is the first concern of this task.

An acceptable mesh creation is an iterative process. All simulation results including electromagnetic, surface heat flux, etc. are highly dependent on the mesh density. That's why the usual procedure is to create a fine mesh in critical areas on the surfaces, while retaining a larger mesh in not so important places of body in order to reduce run time and memory usage. A simple way to achieve this mesh variation is to divide the vacuum volume into sub-volumes depending on the needed local mesh size. In this way, not only the surface mesh can be controlled by sizing areas and lines but the „global" mesh size can be set on the local basis for each sub-volume, resulting in better mesh control.

The use of regular mesh looks favourable for the axisymmetric structures. At the same time during cavity design together with its environments it is not always possible to provide 2D simulations. Again, the most important feature of the mesh adjustment is to control E_{pk}/E_{acc} and B_{pk}/E_{acc} ratio values. The presented plots (Fig.1) show that it is not obvious that the more tense mesh corresponds to the better results. Even more, for such structures the regular mesh might be disadvantageous while the axisymmetric mesh lines will cause inhomogeneous of the field distribution.

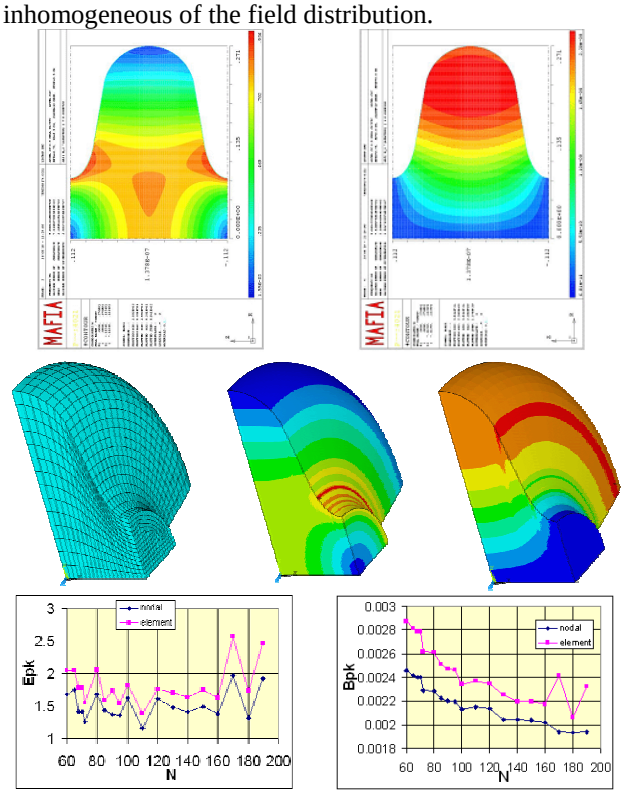

Figure 1: Single-cell elliptic cavity simulations with regular mesh (top row – MAFIA simulations).

This could be eliminated using the auto mesh generation again searching for the best mesh tense (Fig.2). As a rule, only a combination of all possible mesh generation tool adjustments can bring the proper result (Fig.3).

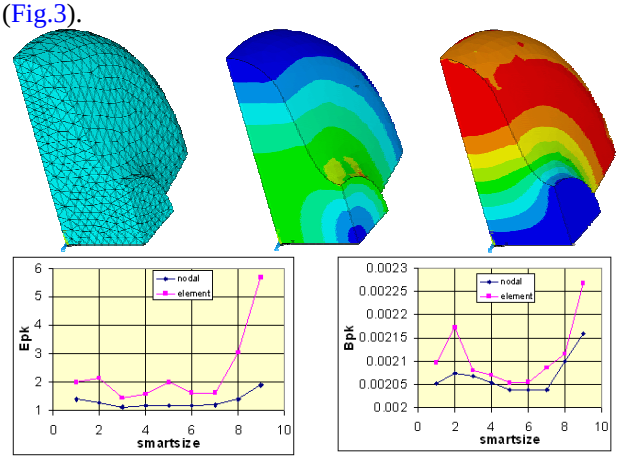

Figure 2: Single-cell elliptic cavity simulations with auto mesh generation (lower "smartsize" corresponds more dense mesh).

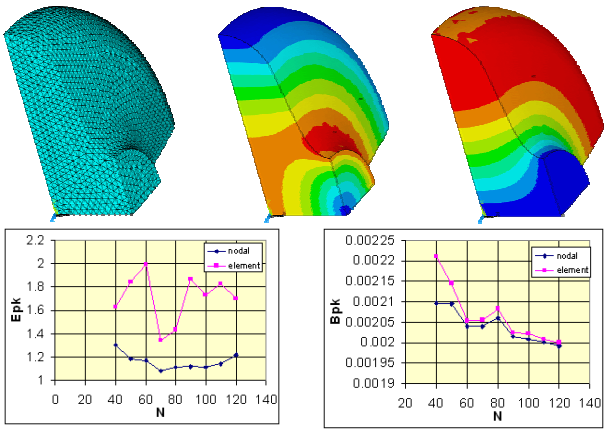

Figure 3: Single-cell elliptic cavity simulations with optimized auto mesh generation.

The same conception of the model meshing is applied to the multi-gap elliptic cavity with the minor mesh modification for the end-cup. Fig.4, Table 1 and Fig.5, Table 2 show the results of the 5-cell cool-down and 1-bar wall pressure simulations [4]. There is a clear difference between single-cell and multi-cell-beam-pipe simulations. The next step is to include the cavity cryo-environments.

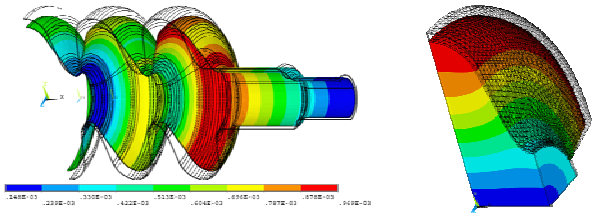

Figure 4: Elliptic cavity deformations by cool-down

Table 1: Elliptic cavity cool-down simulations.

Cool-Down	5-cell cavity	single cell
max displ. [mm]	0.969	0.564
max stress [MPa]	284	22.7
frequency [MHz]	501.5209	502.065
df [kHz]	1500.15	1308.311

The most complicate and computer time consuming are the simulations of the cavity detuning caused by the Lorenz forces. The main advantage of ANSYS codes that through all the calculation procedure they use the same meshed model applying the mesh cell deformations during the structural analysis.

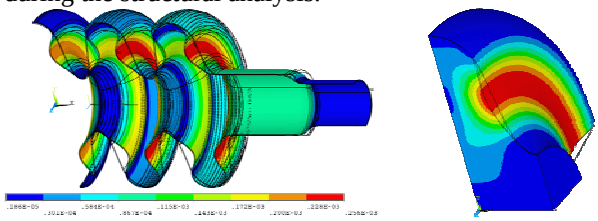

Figure 5: Elliptic cavity deformations under 1 bar wall pressure

Table 2: Elliptic cavity under 1 bar wall pressure.

1 bar pressure	5-cell cavity	single cell
max displ. [mm]	0.256	0.212
max stress [Mpa]	57.8	34.2
frequency [MHz]	501.5209	500.782
df [kHz]	5.728	25.1

The simple cell shape of the elliptic cavity allows using effectively the perturbation method for single cell Lorenz force detuning (LFD) calculations. For this cavity we used 2D electromagnetic fields and Lorenz force pressure calculated with MAFIA, transferred the pressure into ANSYS 2D model, evaluated the structure displacements and calculated LFD. The results are summarized in Table 3.

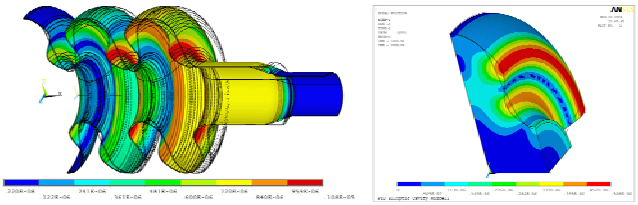

Figure 6: Elliptic cavity deformations by Lorenz forces

Table 3: Elliptic cavity static Lorenz force detuning simulations.

LFD	5-cell	single	exp	single/pert.m.
K_L [Hz/(MV/m)**2]	-3.08	-2.99	-3.72	-3.95

2 HALF-WAVE RESONATOR

The final mesh adjustment should be provided taking into account the real field distribution in the cavity. Since in HWR the magnetic field distribution is not symmetric between inner and outer electrodes the optimal mesh is also should be not symmetric. Fig.7 shows the results of the mesh tune in FZJ HWR. Here every model differs by only one mesh step at the cavity dome.

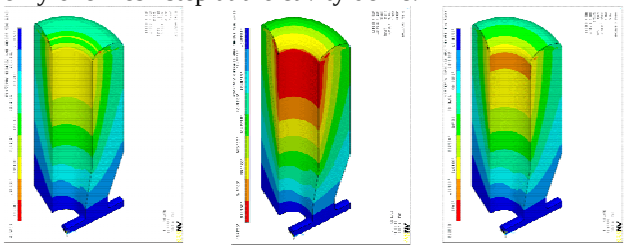

H_{pk}=0.002528 H_{pk}=0.001897 H_{pk}=0.002362

Figure 7: HWR magnetic field distribution with different mesh around B_{pk} region

The good agreement has been detected during relative crosscheck of different simulations and their combination (Table 4). Still, the comparison of the calculated data with measured [5] shows rather large difference (Table 5). The difference of the factor of two in the tuning sensitivity results can be partly explained by the existence of the

uncertainty in the tuner position allocation. The strong dependence of the results on the proper cavity wall thickness can explain the differences for other analyses results (Fig.8).

Table 4: HWR data comparison.

	max displ.	df	K_L
	mm	[Hz]	Hz/(MV/m)**2
1 Bar	0.1	-17698.7	
LFD+1bar	0.101	-17944.9	
(LFD+1bar)-1Bar	0.001	-246.22	-3.8472
LFD	.000994	-243.86	-3.8103

Table 5: HWR data comparison.

	experiment	simulation
f_0@RT [MHz]	160.4	160.2
df after pumping [kHz]	-50	-30
df after cool-down [kHz]	260	370
tuning [kHz/mm]	120	250
LFD [Hz/(MV/m)**2]	6	5

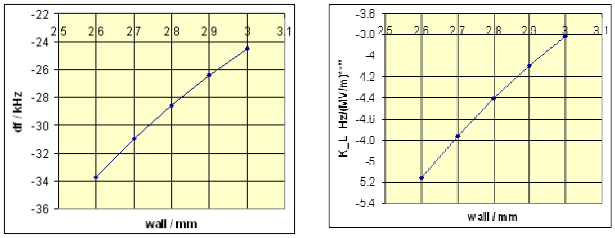

Figure 8: Cavity parameter dependence on wall thickness (left – frequency shift after pumping, right – LFD).

3 TRIPLE-SPOKE CAVITY

The most complicated case for the optimal mesh generation if the location of E_{pk} and B_{pk} in the cavity changes the position during cavity design like in triple-spoke cavity (Fig.9, the dashed line on the plot indicates the moment of E_{pk} location change).

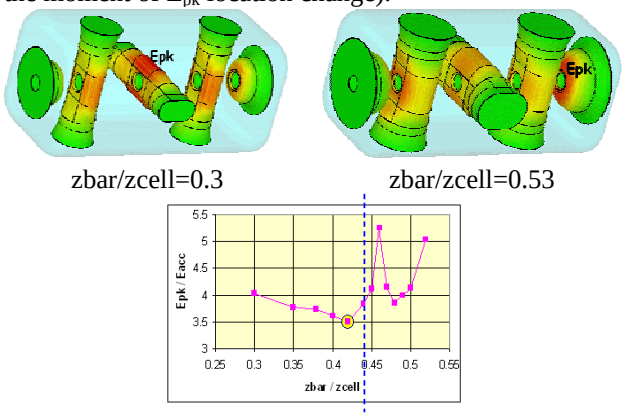

zbar/zcell=0.3 zbar/zcell=0.53

Figure 9: E_{pk} location for different triple-spoke cavity geometries

In this case the use of automesh generation (for instance in MWS) can cause wrong field calculation results (like peaks in the field dependence behaviour). The use of the more dense mesh also doesn't guarantee the better results (Fig.10).

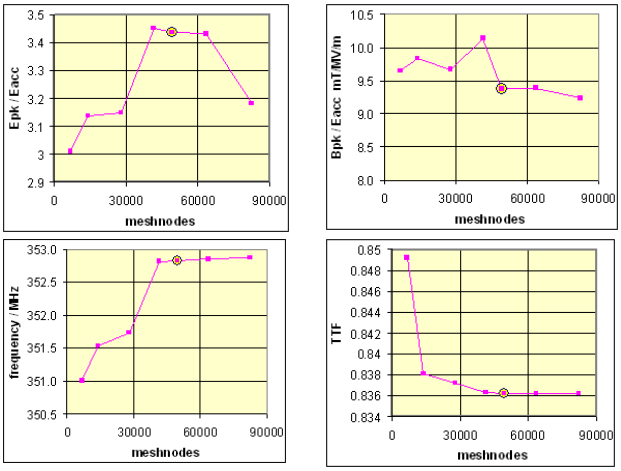

Figure 10: Cavity parameter dependences on mesh dense.

At the same time the use of the manual mesh generation (like in MAFIA) could produce the controlled mesh in the region of interest and more reliable results (Fig.11, e-field region mesh optimized, b-field region mesh not optimized). It has been noticed that MAFIA usually calculates at least 20% lower values for peak fields.

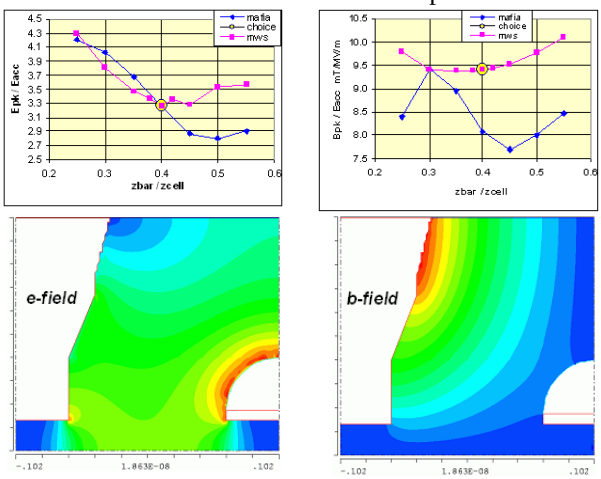

Figure 11: Mesh optimisation in MAFIA

The simulation results of the cavity cool-down frequency shift strong differ from the measured (Table 6). Fig.12 shows that after cool-down cavity contraction mainly magnetic field region is affected. The simulation of the cavity frequency and b-field distribution with MWS and ANSYS show very similar results.

Table 6: Triple-spoke cavity cool-down.

	max displ.	max stress	df	Freq
	[mm]	[MPa]	[kHz]	[MHz]
bp fixed	0.272	83.6	2421.5	758.81
bp free	0.273	0.132	1559.8	757.94
bp free / exp			844	760.08

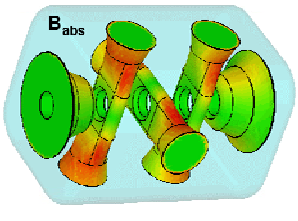

MWS - Freq= 762.7 MHz

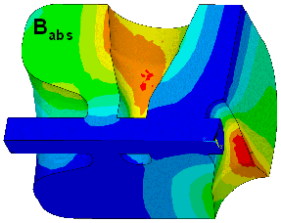

ANSYS - Freq= 757.6 MHz

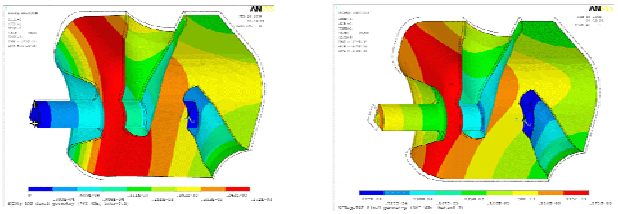

Figure 12: Triple-spoke cavity cool-down simulations

The accuracy of simulations very much depends on the accurate description of the cavity cryo-environments in the simulation model. Still, it is rather difficult during cavity design to predict a priory the future cavity constrains in the cryostat. Since nearly always the cavity is supported with certain stiffening by the beam ports (might be with anything else additionally) we provide the cavity simulations for two extreme cases – with beam pipes completely fixed and absolutely free.

Another uncertain aspect that affects the simulation results is the cavity wall thickness. During the manufacture process the wall thickness becomes not homogeneous and can differ much from the original niobium sheets. Fig.13 shows the simulation results of the wall 1 bar pressure and the resulted frequency shift depending on cavity wall thickness. The different behaviour of the curves for fixed/free beam ports is a result of the stronger frequency shift dependence on the cavity end gap capacitance change than magnetic field volume deformation.

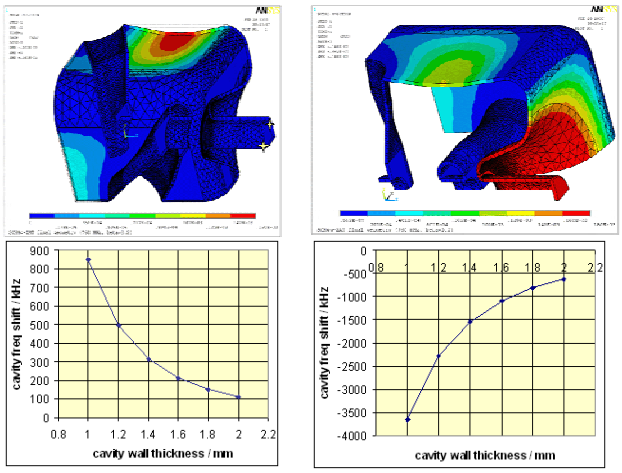

Figure 13: Triple-spoke cavity 1 Bar pressure simulations

Table 7 summarizes the results of cavity cool-down, pumping and their combination simulations. The calculated frequency shifts correspond to each other within simulations but strong differ from the measured.

Table 7: Triple-spoke cavity 1 bar wall pressure simulations.

	Cool-down +1 bar	Cool-down	1 Bar
beam pipes fixed			
Freq [MHz]	758.9	758.79	756.494
df [kHz]	2519.07	2405.11	110.2
max displ.[mm]	0.382	0.271	0.16
max stress [MPa]	46	83	90.5
beam pipes free			
Freq [MHz]	757.31	757.93	755.77
df [kHz]	929	1549.1	-617.64
max displ.[mm]	0.394	0.271	0.18
max stress [Mpa]	79.5	0.132	79.5
beam pipes free / experiment			
df [kHz]			-397

On the other hand the calculated and measured data for LFD are close (Table 8). This is rather strange because one could expect the same big error as the cavity volume deformations by 1 bar pressure and Lorenz forces are similar and mainly related to the cavity end cup displacements (Fig.13-14).

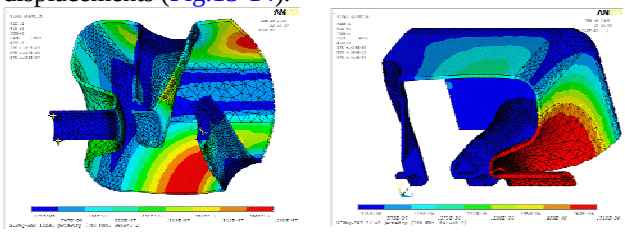

Figure 14: Triple-spoke cavity LFD simulations

Table 8: Triple-spoke cavity LFD.

wall [mm]	Max displ. [mm]	df [Hz]	Freq. [MHz]	K_L Hz/(MV/m)**2
beam pipes fixed				
2	6.60E-05	-428	756.384	-6.681
1	3.98E-04	-2299	756.382	-35.925
beam pipes free				
2	5.16E-04	-2502	756.382	-39.09
1	2.07E-03	-10510	756.374	-164.23
beam pipes free / experiment				
				-175

4 SUMMARY

1. In all three cases LFD simulation data are rather close to the measured.
2. The biggest error for cool-down cavity simulations for both HWR and triple-spoke.
3. Simulation results of 1-bar wall pressure for HWR are rather good. Triple-spoke cavity has small dimensions and high frequency, the small

deformations (but big enough to compare with LFD) result in bigger error.
4. The wall thickness uncertainty brings additional error.
5. It is well known, that LFD measurements can differ much from one measurement to another since they are most sensitive to the cavity constrains in the cryostat. Additionally, the cavity displacements caused by Lorentz forces are within μm's, and the cavity manufacture tolerances usually 100-200 μm. That's why one should expect here the biggest difference between simulation and experimental data.
6. The cavity constrains in the cryostat should be simulated as close to the reality as possible since they can play the dominant role for accuracy of the simulation results.
7. Table 9 summarizes the frequency shifts of all provided simulations. The big cavities with lower frequencies (HWR in our case) can be simulated with better accuracy since all deformations will cause lower relative frequency drifts.
8. The precision of the FEM geometry approximation and eigen-value problem solution for 3D simulation can be already insufficient to determine small values of the frequency shifts.
9. More analyses of different type cavities are required.

Table 9: Cavity frequency shifts.

		Freq. [MHz]	df [kHz]	df / f %
elliptic	cool-down	500	1500	0.3000
	1 Bar	500	5.73	0.0110
	LFD	500	0.6	0.0001
HWR	cool-down	160	370	0.2313
	1 Bar	160	30	0.0188
	LFD	160	0.3	0.0002
triple-spoke	cool-down	760	1549	0.2038
	1 Bar	760	618	0.0813
	LFD	760	5	0.0007

5 ACKNOLEDGEMENTS

We acknowledge the support of the European Community-Research Infrastructure Activity under the FP6 "Structuring the European Research Area" program (CARE, contract number RII3-CT-2003-506395).

6 REFERENCES

[1] MAFIA, MWS are trademarks of CST Inc. www.cst.com.
[2] HFSS is a trademark of ANSOFT Inc. www.ansoft.com.
[3] ANSYS is a trademark of SAS Inc. www.ansys.com.
[4] R. Stassen, private communication.,
[5] R. Stassen et al., "First Results of Pulsed Superconducting Half-Wave Resonators", EPAC'2004, Luzerne, 2004.